

Analysis and mitigation of stimulated Raman scattering effects in OTDR monitored optical link

A.H. Hussein^a, S.B.A. Anas^{a,*}, M.S. Ghazali^a, R. Amran^a, S. Yaakob^a, M.H.A. Bakar^a, K. Khairi^b, A. Ahmad^b, N.A. Ngah^b, S.Z. Muhd-Yassin^b, D.C. Tee^b, Y.I. Go^c

^a Wireless and Photonics Networks Research Centre of Excellence (WiPNET), Department of Computer and Communication Systems Engineering, Faculty of Engineering, Universiti Putra Malaysia, Serdang, 43400, Selangor, Malaysia

^b Telekom Research & Development Sdn Bhd. (TMR&D), TM Innovation Centre, Lingkaran Teknokrat Timur, Cyberjaya, 63000, Selangor, Malaysia

^c School of Engineering and Physical Sciences, Heriot-Watt University, Malaysia, 1, Jalan Venna P5/2, Precinct 5, 63000, Putrajaya, Malaysia

ARTICLE INFO

Keywords:

Optical time-domain reflectometer (OTDR)
Active fiber monitoring
Stimulated Raman scattering (SRS)
Erbium-doped fiber amplifier (EDFA)

ABSTRACT

The co-existence of both traffic signal and optical time-domain reflectometer (OTDR) signal in active fiber monitoring will affect the dynamic range of the OTDR due to backscattered stimulated Raman scattering (SRS). In this paper, a simulation model and hardware experiment are proposed to investigate and mitigate the effects of a backscattered SRS signal on OTDR active fiber monitoring. A basic OTDR active fiber monitoring system based on non-amplified and amplified links was developed, where the effects of SRS backscattered noise, amplification noise, and power depletion were observed. The obtained simulation results indicated that the highest backscattered SRS was contributed by the booster amplifier link configuration, where the amplification of the OTDR signal increased drastically when the signal input power reached 10 dBm. The simulation setup was also used to mitigate the backscattered SRS by placing a chirped fiber Bragg grating (CFBG) at the OTDR to allow only the 1650 nm OTDR signal to be received by the OTDR, leaving other unwanted signals or noise behind. This mitigation successfully reduced other backscattered signals by approximately 4 dB. A proof-of-concept hardware experiment was conducted to test the feasibility of the proposed technique, and the result showed that the distortion in the trace was decreased and the OTDR penalty was also reduced to 0.41 dB.

1. Introduction

Optical time-domain reflectometers (OTDRs) are widely used in fiber communication systems to troubleshoot fiber networks, identify the loss distribution of fibers, evaluate connection losses, and locate the breakpoints (Ito and Manabe, 2016). OTDR monitoring can be done using out-of-service or dark fiber to detect any possible cable intrusion. However, this system lacks accuracy as it can only detect when the fault happens to the out-of-service fiber. In-service or active fiber monitoring has become a powerful enabling tool for an optical network because locating and identifying any source of fault in the network can be done automatically. This monitoring system significantly improves the network management system (NMS) by providing real-time optical infrastructure visibility so that fault detection and localization time are reduced (Rad et al., 2011; VIAVI Solutions, 2018). Stimulated Raman scattering (SRS) transfers power from a shorter to a longer wavelength. As the wavelength spacing increases, the power transfer efficiency increases until it reaches roughly 110 nm, corresponding to the maximum SRS efficiency (Li et al., 2014). Since OTDR uses a

1625/1650 nm wavelength to monitor C-band data traffic, both the traffic signal and the OTDR signal channel separation exactly match the peak Raman gain coefficient of the used single-mode fiber (SMF) (Venter, 0000). Due to the effect of SRS, the data traffic is depleted by the OTDR pulse (Chen and Leblanc, 2004). For live-fiber monitoring, spontaneous Raman scattering, which is generally a negligible feature in transmission systems, becomes a significant limitation (Chen et al., 2007). Despite the low power level of Raman scattering, the OTDR has high sensitivity, and this scattering can considerably reduce the OTDR's dynamic range (Venter, 0000). To overcome the SRS effect in online monitored systems, a solid understanding of the SRS effect between the high-power pulses of OTDR and the traffic is required while deploying OTDR-based live fiber testing (Chen et al., 2007).

Several methods and techniques have been proposed in the literature to investigate and mitigate the SRS effect in an online OTDR monitoring system. Zhang et al. studied the negative effects of SRS on the usage of optical supervisory channel (OSC) and optical time domain reflectometer (OTDR). The OTDR's ability to provide accurate

* Corresponding author.

E-mail address: barirah@upm.edu.my (S.B.A. Anas).

measurements is hindered by the power loss resulting from SRS effects on the monitoring signal. To mitigate this, a precise evaluation of the SRS effect within the tested fiber span must be performed, which is then used to numerically correct the distortion it generated on the OTDR measurement (Zhang et al., 2022). Another study in Kuo et al. (2004) investigated the impact of in-line monitoring with 1650 nm OTDR on 1550 nm distributed fiber Raman amplifier (FRA) transmission systems. The amplified 1650 nm OTDR light distorts the OTDR trace, resulting in inaccurate fiber loss measurements. A study in Kim et al. (2014) investigated the power depletion in dense wavelength division multiplexing (DWDM) signals caused by the OTDR signals with high power in mobile fronthaul. The result shows that when a 1544.53 nm signal co-propagates with a 1655 nm OTDR signal with 20 dBm peak power, the maximum power depletion is 1.1 dB. They proposed to use 1625 nm or 1665 nm wavelength for the OTDR monitoring signal to reduce the SRS power depletion. The papers (Pellegatta et al., 2002; Tsai et al., 2002, 2003) also proposed attenuating the OTDR peak power to mitigate the SRS distortion. However, reducing the OTDR signal power will limit the OTDR performance. Using a narrow-bandwidth tunable OTDR and an optical bandpass filter, the authors in Chen and Leblanc (2004) proposed a simple way to mitigate the degradation of online fiber monitoring. The OTDR penalty imposed by the SRS produced by traffic signals was drastically reduced. According to Chen et al. (2007), Kjeldsen et al. (1997) and Kjeldsen et al. (1996), the SRS-induced depletion is greatly reduced if the OTDR pulses are counter-propagating relative to the traffic signal. The OTDR pulse in counter-propagation takes energy from several parts of the traffic signal, resulting in less SRS depletion. However, this limits the use of an OTDR to monitor fibers carrying incoming traffic. A numerical and experimental study of probe pulse deformation caused by distributed Raman amplification in OTDR-based sensing systems was reported in Wang et al. (2023). The results showed that using a smaller Raman gain coefficient can reduce pump depletion and mitigate the probe pulse deformation by detuning the pump and probe frequency shift.

In this paper, a simulation model and hardware experiment are proposed to investigate and mitigate the impact of SRS on the OTDR-monitored Erbium-doped fiber amplifier (EDFA) amplified link to the data-modulated traffic signals. By creating a simple OTDR active fiber monitoring system, the SRS backscattered noise, amplification noise, and power depletion are observed for both non-amplified and amplified links. A chirped fiber Bragg grating (CFBG) was used to mitigate the backscattered SRS, and it successfully reduced other backscattered signals by approximately 4 dB. A proof-of-concept hardware experiment was performed to test the feasibility of the proposed technique. By mitigating the backscattered noise, the distortion in the trace and the OTDR penalty were reduced, improving OTDR active fiber monitoring performance.

2. Power depletion induced by SRS

In SRS, the low-frequency channels are amplified at the expense of the higher frequency ones. Due to the Raman coefficient frequency response, this effect is insignificant at bandwidth under 5 THz. When the bandwidth of the signal is increased, the key nonlinear phenomenon that will limit the capacity of optical communication systems will be the SRS (Paz and Saavedra, 2021). Assuming N channels that are equally spaced with a channel spacing of $\Delta\nu$ (Hz), the SRS will have the most impact on the channel with the shortest wavelength. Channel 1 power loss D is given by :

$$D = \sum_{i=1}^{N-1} \frac{\lambda_i}{\lambda_o} \frac{P_i g_i L_e}{2A} \quad (1)$$

where P_i is the injected power in i th channel, λ_i is the wavelength of i th channel, λ_o is the wavelength of channel 1, N is the number of channels, g_i is the Raman gain coefficient coupling the i th and channel 1, and A

is the effective core area. L_e is the effective length of the fiber given as:

$$L_e = \frac{1 - e^{-\alpha L}}{\alpha} \quad (2)$$

where α is the fiber loss coefficient, and L is the actual fiber length.

For WDM systems with EDFA, it is assumed that there are n EDFAs with gain K_i ($i=1 \dots n$), and N channels. $S_i(0)$ ($i=1 \dots N$) (mW) is signal power injected to the input port of the EDFA. The equation governing the propagation of multi wavelength signals can then be written as Xiang et al. (1996):

$$\frac{dS_i(z)}{dz} = [-\alpha(z) + \sum_{j=1}^{i-1} \frac{g_{ji} S_j(z)}{2A} - \sum_{j=i+1}^N \frac{\lambda_j g_{ij} S_j(z)}{\lambda_i 2A}] S_i(z) \quad (3)$$

Where n is the number of EDFAs, $S_{i(0)}$ ($i = 1, 2, \dots, N$) is the signal power, be injected at $z = 0$ along $+z$ direction. $\alpha(z)$ is the loss coefficient of the fiber, A is the effective core area. g_{ji} is the Raman gain coefficient coupling the channels i and j . The wavelengths of i th channel and j th channel are denoted λ_i and λ_j . Since the loss of energy will be highest in channel 1, only the power depletion of channel 1 needs to be determined such that:

$$\frac{dS_1(z)}{dz} = [-\alpha(z) - \sum_{j=2}^N \frac{\lambda_j}{\lambda_1} \frac{g_{1j} S_j(z)}{2A}] S_1(z) \quad (4)$$

Integrating from $z = 0$ to $z = L$, we get:

$$\frac{10 \log S_1(L)}{S_1(0)} = (10 \ln) K - (10 \ln) \alpha L - (10 \ln) D \quad (5)$$

where $K = \sum k_i$ which is total gain of EDFAs. The first term in Eq. (5) expresses the total gain provided by all EDFAs. The second term represents the signal loss experienced due to imperfections in the fiber itself. Finally, the third term expresses the power depletion in channel 1 caused by SRS which is given by:

$$D = \sum_{j=2}^N \frac{\lambda_j}{\lambda_1} \frac{g_{1j}}{2A} \int_0^L S_j(z) dz \quad (6)$$

To calculate channel 1 power penalty, the effect of SRS in other channels can be neglected.

$$S_j(z) = S_j(0) \cdot \exp[K(z) - \alpha z], (j > 1) \quad (7)$$

$$\int_0^L S_j(z) dz = S_j(0) \int_0^L e^{[K(z) - \alpha z]} dz \quad (8)$$

Let us consider a WDM system with n EDFAs and with gain $k_i = K$, and spacing $L_i = L$. Integrating from $z = 0$ to $z = L_1$, We let $K(z) = k_1$ and $L = L_1$. Integrating from $z = 0$ to $z = L_2$, We Let $K(z) = k_1 + k_2$ and $L = L_2$.

So, the integration of $e^{K(z) - \alpha z}$ from $z = 0$ to $z = L$ is:

$$\int_0^L e^{[K(z) - \alpha z]} dz = \frac{e^{k_1 - \alpha L_1} - e^{k_1} + e^{k_1 + k_2 - \alpha L_2} \dots e^{\sum K_i - \alpha L} - e^{\sum k_i - \alpha L_{n-1}}}{-(\alpha)} \quad (9)$$

so,

$$\int_0^L S_j(z) dz = S_j(0) \left[\frac{e^{k_1 - \alpha L_1} - e^{k_1} + e^{k_1 + k_2 - \alpha L_2} + \dots + e^{\sum K_i - \alpha L} - e^{\sum k_i - \alpha L_{n-1}}}{-(\alpha)} \right] \quad (10)$$

We take L_e which is the effective length calculated as follows:

$$L_e = \frac{e^{k_1 - \alpha L_1} - e^{k_1} + e^{k_1 + k_2 - \alpha L_2} + \dots + e^{\sum K_i - \alpha L} - e^{\sum k_i - \alpha L_{n-1}}}{-(\alpha)} \quad (11)$$

Assuming that $S_j(0)$ is identical for all channels, $S_j(0)$ and considering $\lambda_j \approx \lambda_1$,

$$D = \frac{\Delta\nu S_j(0) g_p}{3 \times 10^{13} \cdot A} \frac{N(N-1)}{2} L_e \quad (12)$$

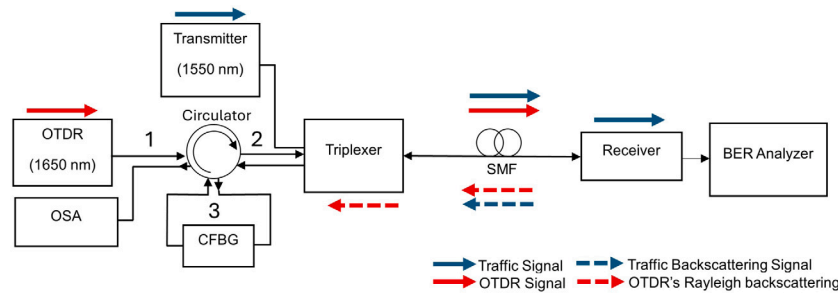


Fig. 1. Simulation setup block diagram.

For typical parameters, $A = 5 \times 10^{-11} \text{ m}^2$ and peak Raman gain $g_P = 6 \times 10^{-14} \text{ m/W}$, $\Delta\nu$ is the channel spacing, the power penalty caused by the SRS is given by:

$$D_{dB} = 10 \ln D = 8.68 \times 10^{-17} \Delta\nu S_j(0) N(N-1) L_e \quad (13)$$

As shown in Eq. (13), the penalty caused by the SRS depends on the length of the fiber, EDFA gain and the input power. The inclusion of EDFA will increase the power depletion caused by the SRS.

3. Experimental and simulation setup

To investigate the effects of SRS in OTDR active fiber monitoring, the non-amplified link and the booster amplifier were separately examined in OptiSystem Version 17, as shown in Fig. 1. At the transmitter, a traffic signal with a wavelength of 1550 nm was combined with a 1650 nm OTDR signal using a triplexer. For the booster configuration, the EDFA with 10 dB gain was placed just after the transmitter to amplify the signal before injecting it into the fiber. The 1650 nm and 1550 nm backscattered signals were received at the triplexer, suppressing the signals ranging from 1540 nm to 1560 nm and allowing other wavelengths, including 1650 nm to pass through. The 1650 nm backscattered signal was passed through the circulator and received at the OTDR. The backscattered signal was measured using an optical spectrum analyzer (OSA) and optical power meter without a CFBG filter. To mitigate the backscattered SRS, the backscattered signal from Port 1650 nm of the triplexer will go through Port 2 of the circulator and come out from Port 3. It will then be filtered by the CFBG, which reflects 1650 nm wavelength to the circulator. The OSA then receives the reflected signal from Port 1 of the circulator. Since uniform FBG offers a narrow reflection band, we chose CFBG for its wider reflection bandwidth. The OTDR subsystem consists of CW Laser, measured pulse sequence, and Mach-Zehnder modulator (MZM). The MZM controls the amplitude of the CW laser based on the input in the Measured Pulse Sequence to generate the OTDR signal. The triplexer subsystem consists of an ideal multiplexer and a reflective filter that functions as a bidirectional triplexer. The center wavelength of the reflective filter was set to 1550 nm with a bandwidth of 20 nm. The receiver subsystem converts light signal to electrical signal and consists of Butterworth optical filter, PIN photodiode, and low pass Bessel filter. The traffic input power was varied from -10 dBm to 20 dBm . A bidirectional fiber was used since it was able to simulate the Rayleigh scattering and Raman scattering behavior ranging from 0 km to 100 km. Parameter values used for the SRS investigation are shown in Table 1.

The experimental setups similar to the simulation design are shown in Fig. 2 to test the feasibility of the proposed technique. Two setups were investigated: connection establishment using a tunable laser source (TLS) and connection establishment between two transmitting nodes of the metropolitan-Ethernet (Metro-E) network. Fig. 2(a) shows the setup for 80 km active fiber monitoring by using TLS to transmit the data traffic. A 2x2 wavelength independent optical power splitter with a 50:50 ratio was used to divide power at port 1650 nm to enable the use of an optical spectrum analyzer (OSA) at the OTDR. OSA at

Table 1
System parameters.

Parameter	Value	
SMF	Effective area of core A_{eff} (μm^2)	80
	Dispersion (ps/nm/km)	16.75
	Dispersion slope (ps/nm ² /km)	0.075
	Attenuation coefficient (dB/km)	0.2
	Rayleigh Backscattering/km	50e-6
Length (km)	40, 80	
Signal	Input power (dBm)	4
	Wavelength (nm)	1550
OTDR	Wavelength (nm)	1650
	Power (dBm)	-3.5
	Pulse width (ns)	100
EDFA	Gain (dB)	10

the OTDR was used to observe the backscattered signal power and spectrum received by the OTDR, while OSA at the receiving end was used to observe the output power and spectrum after propagating the 80 km SMF. The system performance was analyzed using the obtained received power and OTDR trace. The TLS input power ranges from 0 dBm to 7 dBm.

Fig. 2(b) shows the connection of OTDR active fiber monitoring using two D-Link DGS-1510-28 SmartPro switches with small form-factor pluggable (SFP) + 40 km 1550 nm transceivers at 10 Gbps transmission rates. The OTDR being used was Viavi Smart OTDR Handheld Fiber Tester. In the Metro-E network, the transmission utilized a 1550 nm operating wavelength for transmission and receiving in two separate fibers. The backscattered signal mitigation setup was done on one bidirectional transmission link by placing the filter just after the OTDR. This setup demonstrates a co-propagating configuration where the OTDR and transmitter of Switch A are located at the same end. Since the transmitter power of the Metro-E switch is fixed, a variable optical attenuator (VOA) was used to vary the transmitter power. The setup parameters are shown in Table 1.

4. Results and discussions

In this section, the obtained results from simulation and the hardware experiment are discussed.

4.1. Simulation results

The effect of SRS is investigated in terms of the output power of the OTDR signal, the output power of the traffic signal, and the backscattered signal power. The OSA spectrum of the backward propagating signal at the OTDR receiver is shown in Fig. 3. For the non-amplified link, as shown in Fig. 3(a), there was no ASE noise generated, and the traffic input power of 4 dBm was not sufficient to induce the SRS. However, for the booster amplified link in Fig. 3(b), it can be noticed that ASE noise and SRS are generated. The green color represents the Stokes scattering generated by the SRS, while the blue color is the ASE

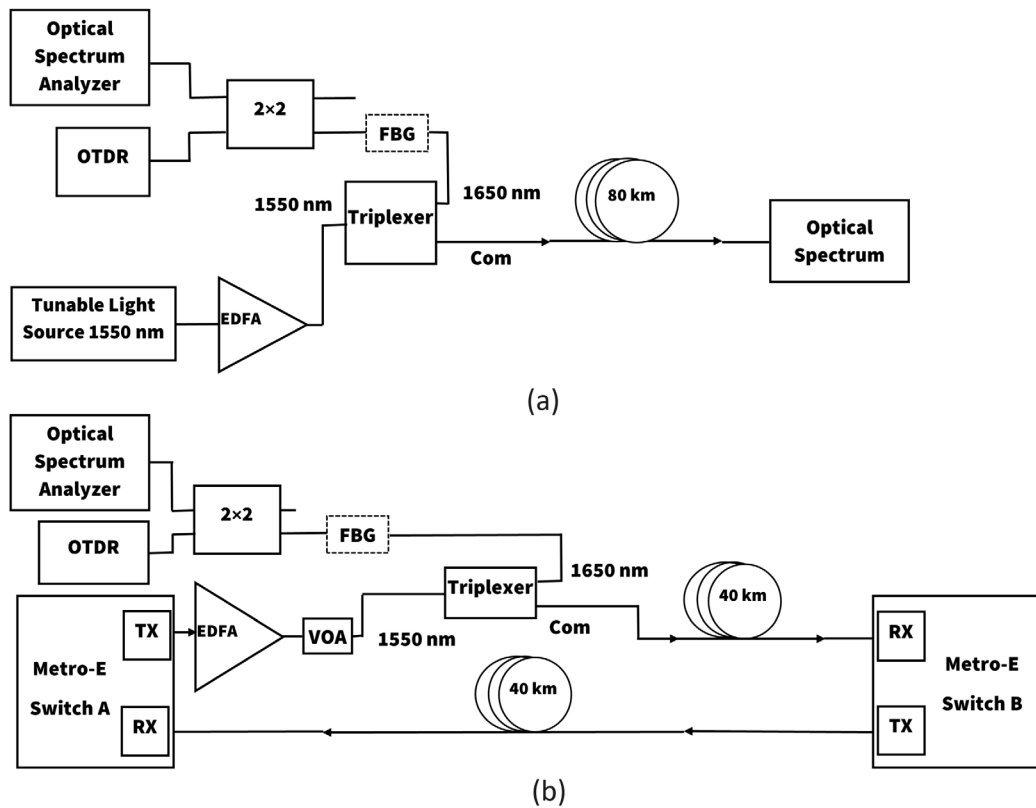


Fig. 2. Setup for (a) 80 km unidirectional link with OTDR active fiber monitoring using TLS (b) 40 km bidirectional link with OTDR active fiber monitoring in Metro-E network.

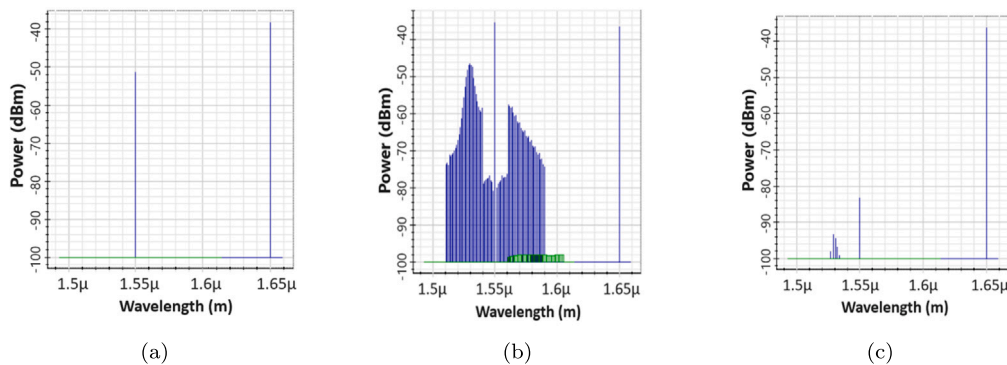


Fig. 3. Spectrum of back-reflected signal for (a) non-amplified (b) booster amplifier configurations (c) booster amplifier with CFBG.

noise. Fig. 3(c) shows the OSA spectrum after the successful mitigation of SRS using CFBG. The power difference between OTDR signal and other backscattered signals was higher than 20 dB, demonstrating the effectiveness of CFBG in mitigating SRS.

The effect of traffic input power on the OTDR output power is shown in Fig. 4(a). There is a significant increase in OTDR output power for the booster amplifier, and it becomes serious when traffic input power reaches 10 dBm and above. The non-amplified link also shows notable increases after reaching 16 dBm, but not as high as the booster amplifier link. The SRS effect starts increasing when traffic input power is 10 dBm for the booster amplifier link and 16 dBm for the non-amplified link. Fig. 4(b) shows the effect of traffic input power on the backscattered power. As can be seen, the booster amplifier link contributes the highest backscattered OTDR power, while the non-amplified link indicates similar backscattered OTDR power. The backscattered OTDR power for the booster amplifier link was high due to the inclusion of both backscattered ASE noise and backscattered SRS.

The effect of OTDR input power to the traffic output power is also investigated. Fig. 5(a) shows that a slight reduction in the traffic output power started to occur when the OTDR input power was higher than ten dBm. The power reduction occurred, and the energy was transferred to the longer wavelength due to the SRS effect. The OTDR input power below 5 dBm did not affect the traffic signal much because it is still below the traffic input power, which is 5 dBm. Fig. 5(b) compares backscattered OTDR power with and without the CFBG filter. At a traffic input power of 4 dBm, the CFBG filter reduced other backscattered signals approximately by 4 dB and left the OTDR signal only at -36 dBm, which corresponds to the peak power of the OTDR signal in the OSA spectrum.

4.2. Experimental results

The obtained results from SRS mitigation setup are discussed in this section.

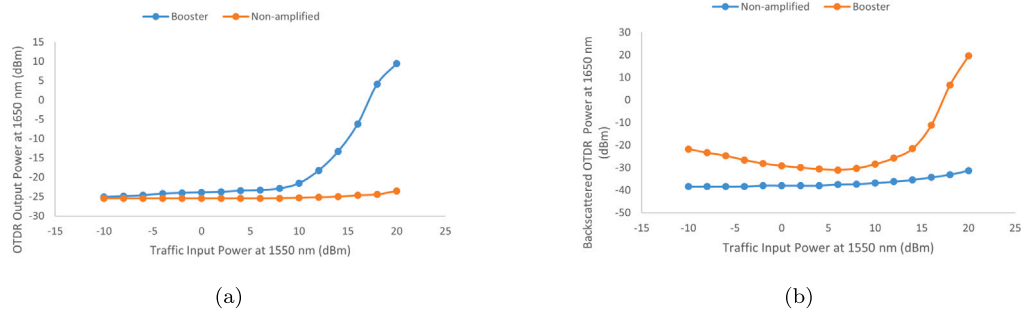


Fig. 4. Traffic input power versus (a) OTDR output power (b) backscattered OTDR Power.

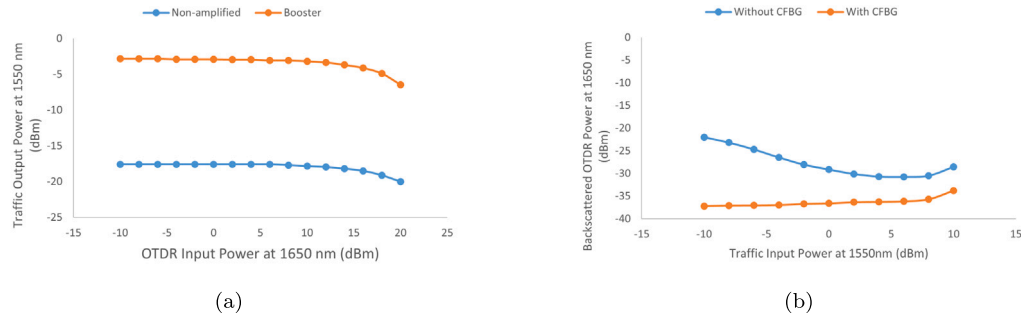


Fig. 5. Traffic input power versus (a) OTDR output power (b) backscattered OTDR Power.

4.2.1. OTDR trace for 80 km unidirectional link with OTDR active fiber monitoring using 1550 nm TLS

The effect of SRS on OTDR trace is investigated for 80 km active fiber monitoring by using TLS as a traffic signal. Fig. 6(a) states the reference trace in which the TLS was turned off. The numbering in the trace indicates where the fiber was connected using fiber connectors. The reference trace ended at -24.8 dB. Fig. 6(b) shows the OTDR trace where the 4 dBm TLS was amplified using an Erbium-doped fiber amplifier (EDFA) with a 10 dB gain booster amplifier, and the trace ended at -28.2 dB. As expected, the booster amplifier setup shows distortion in the trace when the SMF distance reaches 70 km with an OTDR penalty of about 3.4 dB. OTDR penalty determines how much the measurement range is reduced. Fig. 6(c) shows the trace where the FBG filter was used at the OTDR, which ends at -25.21 dB. The OTDR penalty was reduced to 0.41 dB, and the distortion in the trace was minimized. The use of the FBG filter at the OTDR significantly improves the measurement range by mitigating the unwanted backscattered signal.

Fig. 7(a) shows the acquired OSA spectrum which was placed at the OTDR for booster amplifier setup. It can be noticed that the triplexer filter could not completely remove wavelengths other than 1650 nm. Besides backscattered ASE and SRS, the high-power backscattered traffic at 1550 nm also affects and distorts the OTDR trace. Fig. 7(b) shows the OSA spectrum where an FBG filter with a 1550 nm wavelength was placed at the OTDR. The high-power backscattered traffic signal was suppressed from -5.2 dBm to -65.40 dBm. This huge reduction enhanced the OTDR trace for booster amplifier setup, thereby improving signal clarity as can be seen in Fig. 7(b).

4.2.2. OTDR trace for 40 km bidirectional link with OTDR active fiber monitoring in Metro-E network

Figs. 8(a) and 8(b) show the OTDR trace in 40 km link OTDR active fiber monitoring in the Metro-E network without amplifier and amplified link using EDFA with 10 dB gain of booster amplifier. These two traces indicate a similar end, which is at approximately -13 dB. However, there was small difference in the traces when reaching 35 km, where the booster amplifier setup consists of minor distortion compared to the non-amplified setup. Other than that, the dynamic range was also

reduced as can be seen at the noise level. The booster amplifier setup had no severe distortion compared to the 80 km unidirectional link using 1550 nm TLS with the booster amplifier due to the different fiber lengths. The fiber length plays an important role in the backscattered power. If the fiber length is reduced, the backscattered noise is also reduced.

Figs. 9(a) and 9(b) depict the OSA spectrum for the 40 km link of OTDR active fiber monitoring in the Metro-E network for non-amplified setup and for booster amplifier setup received by the OTDR, respectively. In non-amplified setup, the spectrum only contains backscattered traffic signal at 1543 nm and backscattered OTDR signal at 1650 nm, while the spectrum for booster amplified setup contains backscattered noise and falls within the 1650 nm OTDR signal range. That means the backscattered noise was combined with the backscattered OTDR signal received by the OTDR.

5. Conclusion

The investigation and mitigation of backscattered SRS signals in OTDR active fiber monitoring are demonstrated in this paper. For the simulation setup, the booster amplifier link contributed the most, generating backscattered SRS and ASE noise at the OTDR. In addition, the OTDR trace for the booster amplifier setup in 80 km unidirectional link with OTDR active fiber monitoring using TLS shows that there is a distortion in the trace when the SMF distance reaches 70 km with an OTDR penalty of about 3.4 dB. Meanwhile, the non-amplified link indicates a similar trace to the reference trace. Moreover, the OTDR trace for booster amplifier setup in a 40 km bidirectional link with OTDR active fiber monitoring in the Metro-E network also indicates minor distortion when it reaches 35 km distance. The mitigation of the backscattered signal was then performed on the booster amplifier setup, and the OTDR penalty was significantly reduced from 3.4 dB to 0.41 dB. This will give an advantage in accurate and fast detection over the traditional troubleshooting and passive monitoring system counterpart. Future investigations will focus on examining CFBG's effectiveness in suppressing the SRS effect under high-power conditions.

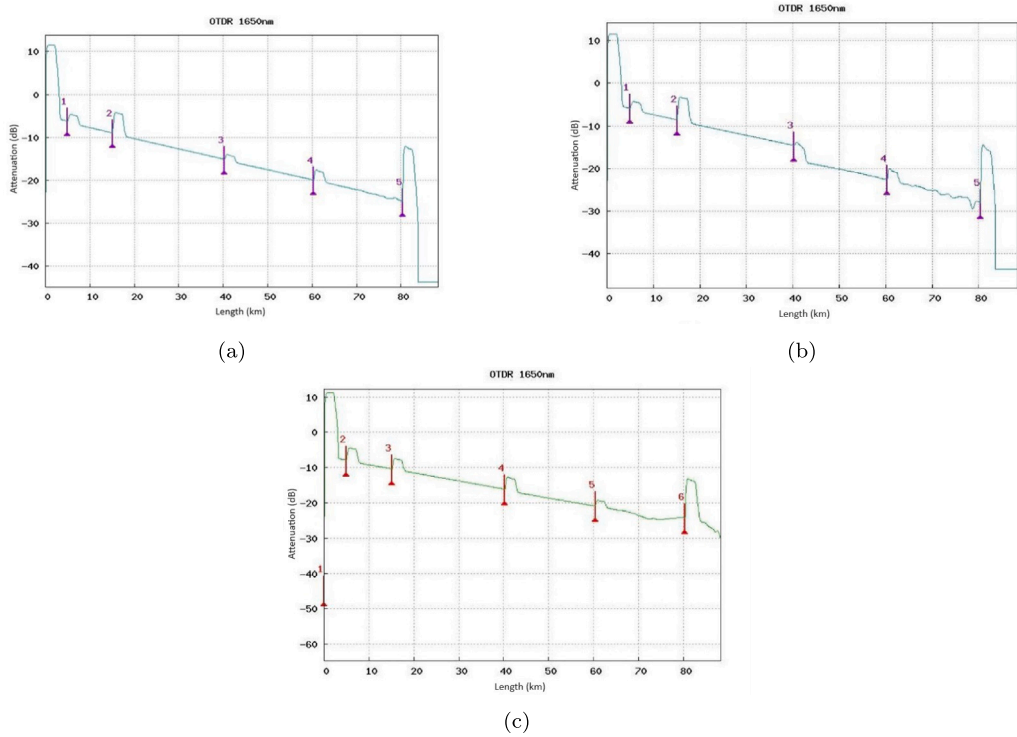


Fig. 6. OTDR trace with 4 dBm TLS at 1550 nm amplified by 10 dB gain EDFA (booster amplifier setup) (a) Reference OTDR trace (b) without FBG filter (c) with FBG filter.

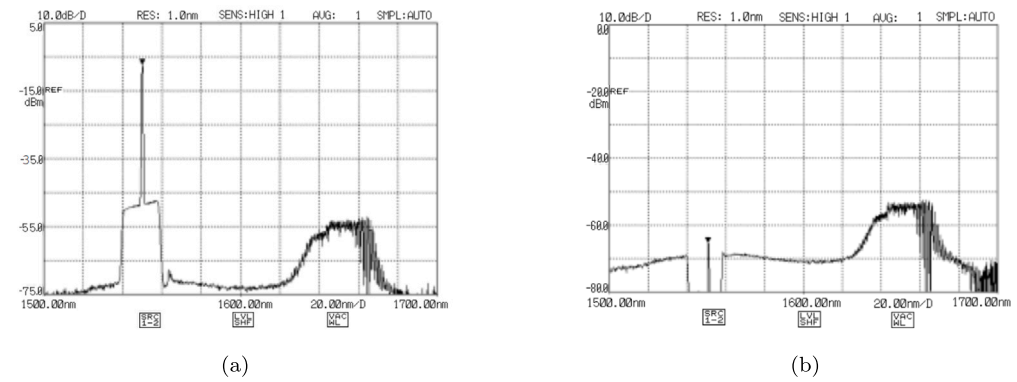


Fig. 7. OSA spectrum for 80 km OTDR active fiber monitoring (a) without FBG (b) with FBG.

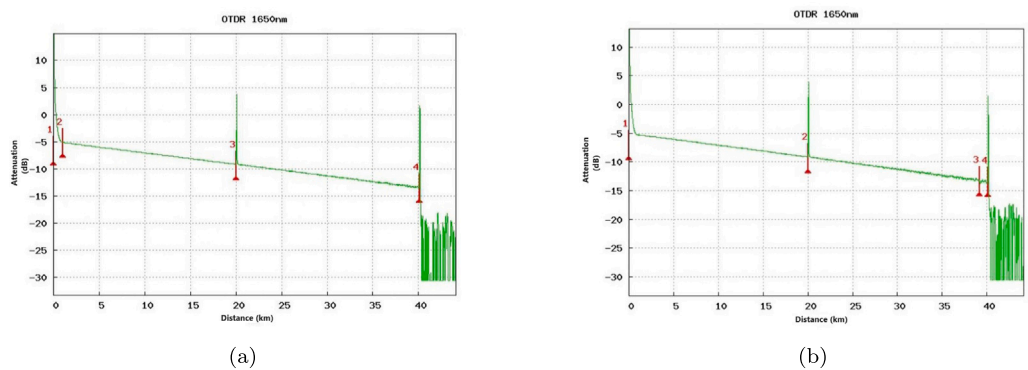


Fig. 8. OTDR trace for 40 km bidirectional link with OTDR active fiber monitoring in Metro-E network (a) non-amplified setup (b) amplified setup.

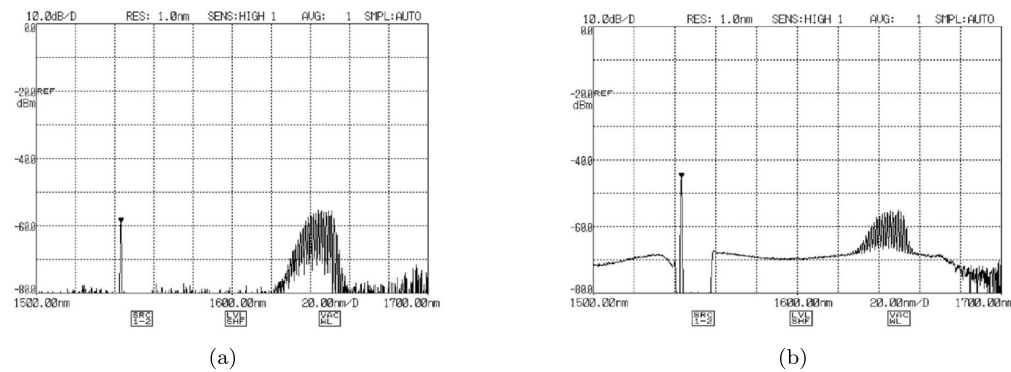


Fig. 9. OSA spectrum for 40 km bidirectional link with OTDR active fiber monitoring in Metro-E network (a) non-amplified (b) amplified.

Funding

This work is funded by Fundamental Research Grant Scheme (FRGS), Ministry of Higher Education, Malaysia, No. FRGS/1/2020/TK0/UPM/02/10.

CRedit authorship contribution statement

A.H. Hussein: Writing – review & editing, Writing – original draft, Software, Methodology, Formal analysis, Data curation, Conceptualization. **S.B.A. Anas:** Writing – review & editing, Validation, Supervision, Project administration, Methodology, Funding acquisition, Conceptualization. **M.S. Ghazali:** Conceptualization. **R. Amran:** Software. **S. Yaakob:** Writing – review & editing, Supervision. **M.H.A. Bakar:** Supervision. **K. Khairi:** Supervision. **A. Ahmad:** Writing – review & editing. **N.A. Ngah:** Writing – review & editing. **S.Z. Muhd-Yassin:** Writing – review & editing. **D.C. Tee:** Writing – review & editing. **Y.I. Go:** Writing – review & editing.

Declaration of competing interest

The authors declare that they have no known competing financial interests or personal relationships that could have appeared to influence the work reported in this paper.

Data availability

Data will be made available on request.

References

- Chen, H., Leblanc, M., 2004. Reduction of the impairment of online OTDR monitoring by use of a narrow bandwidth OTDR and an optical bandpass filter. *IEEE Photonics Technol. Lett.* 16 (9), 2198–2200.
- Chen, H., Leblanc, M., Plomteux, O., 2007. Live-Fiber OTDR Testing: Traffic and Measurement Impairments. EXFO Electro-Optical Engineering Inc, pp. 1–7.
- Ito, F., Manabe, T., 2016. Recent developments of fiber diagnosis technologies in optical communication. *J. Lightwave Technol.* 35 (16), 3473–3482.
- Kim, E.-S., Lee, H.H., Lee, J.C., Lee, S.S., 2014. SRS induced power depletions of WDM signals by a high power OTDR signal in mobile fronthauls. In: 2014 12th International Conference on Optical Internet 2014. COIN, IEEE, pp. 1–2.

- Kjeldsen, P.M., Øbro, M., Madsen, J., Nielsen, S., 1996. SRS induced depletion of 1540 nm signal co-propagating with 1630 nm OTDR pulses. *Electron. Lett.* 32 (20), 1914–1916.
- Kjeldsen, P., Øbro, M., Madsen, J., Nielsen, S., 1997. Bit-error-rate degradation due to on-line OTDR monitoring above 1.6/spl mu/m. In: *Proceedings of Optical Fiber Communication Conference*. IEEE, pp. 95–96.
- Kuo, I.-Y., Tsai, S.-C., Mi, H.-P., Chen, Y.-K., 2004. Probe-trace distortion of 1.65 μm optical time-domain reflectometry in on-line monitoring 1.55 μm fiber Raman amplifier transmission system. *Japan. J. Appl. Phys.* 43 (1R), 156.
- Li, J., Bi, M., He, H., Hu, W., 2014. Suppression of SRS induced crosstalk in RF-video overlay TWDM-PON system using dicode coding. *Opt. Express* 22 (18), 21192–21198.
- Paz, E., Saavedra, G., 2021. Impact of stimulated Raman scattering on ultrawideband systems. In: *2021 IEEE Photonics Society Summer Topicals Meeting Series*. SUM, IEEE, pp. 1–2.
- Pellegatta, M., Monguzzi, M., Mazzaresse, A., Zucchetti, A., 2002. Fiber networks maintenance in the all-optical network era. In: *NOMS 2002. IEEE/IFIP Network Operations and Management Symposium*. Management Solutions for the New Communications World (Cat. No. 02CH37327). IEEE, pp. 855–868.
- Rad, M.M., Fouli, K., Fathallah, H.A., Rusch, L.A., Maier, M., 2011. Passive optical network monitoring: challenges and requirements. *IEEE Commun. Mag.* 49 (2), s45–S52.
- Tsai, S.-C., Huang, M.-H., Chen, Y.-K., 2002. Stimulated Raman scattering-induced baseband video distortion due to 1.65- μm OTDR online monitoring in 1.55- μm AM-VSB CATV system. *IEEE Photonics Technol. Lett.* 14 (7), 1016–1018.
- Tsai, S.-C., Tu, Y.-K., Chen, Y.-K., 2003. Countermeasures of stimulated-Raman-scattering-induced video distortion in 1.65 μm optical time-domain reflectometer on-line monitoring 1.55 μm cable television system. *Japan. J. Appl. Phys.* 42 (7R), 4349.
- Venter, M.G.a.M., 0000. In-Service OTDR Monitoring and Mitigating the Effects of Raman Scattering, <https://www.lightwaveonline.com/test/networktest/article/16667976/in-service-otdr-monitoring-and-mitigating-the-effects-of-raman-scattering>.
- VIAMI Solutions, 2018. Monitoring Raman Amplified Optical Links While In Service. Tech. Rep., VIAMI Solutions.
- Wang, Z., Vandborg, M.H., Joy, T., Mathew, N.M., Grüner-Nielsen, L., Rishøj, L.S., Christensen, J.B., Jostmeier, T., Marx, B., Hill, W., et al., 2023. Mitigating probe pulse deformation in Raman amplification in OTDR fiber sensing systems. *Opt. Express* 31 (7), 11457–11470.
- Xiang, Q., Xu, A., Wu, D., Xie, L., 1996. The calculation of power penalty in "WDM+EDFA" system due to stimulated Raman scattering. *Int. J. High Speed Electron. Syst.* 7 (03), 367–372.
- Zhang, C., Liu, X., Li, J., Zhang, A., Liu, H., Feng, L., Lv, K., Liao, S., Chang, Z., Zhang, J., 2022. Optical layer impairments and their mitigation in C+ L+ S+ E+ O multi-band optical networks with G. 652 and loss-minimized G. 654 fibers. *J. Lightwave Technol.* 40 (11), 3415–3424.